Green function theory versus quantum Monte Carlo calculations for thin magnetic films

S. Henning,* F. Körmann, J. Kienert, and W. Nolting
Lehrstuhl Festkörpertheorie, Institut für Physik, Humboldt-Universität zu Berlin, Newtonstrasse 15, 12489 Berlin, Germany

S. Schwieger
Technische Universität Ilmenau, Theoretische Physik I, Postfach 10 05 65, 98684 Ilmenau, Germany
(Received 17 October 2006; revised manuscript received 28 February 2007; published 1 June 2007)

In this work we compare numerically exact quantum Monte Carlo (QMC) calculations and Green function theory (GFT) calculations of thin ferromagnetic films including second-order anisotropies. Thereby, we concentrate on easy-plane systems, i.e., systems for which the anisotropy favors a magnetization parallel to the film plane. We discuss these systems in perpendicular external field, i.e., B parallel to the film normal. GFT results are in good agreement with QMC for high enough fields and temperatures. Below a critical field or a critical temperature, no collinear stable magnetization exists in GFT. On the other hand, QMC gives finite magnetization even below those critical values. This indicates that there occurs a transition from noncollinear to collinear configurations with increasing field or temperature. For slightly tilted external fields, a rotation of magnetization from out-of-plane to in-plane orientation is found with decreasing temperature.

DOI: 10.1103/PhysRevB.75.214401 PACS number(s): 75.10.Jm, 75.40.Mg, 75.70.Ak, 75.30.Gw

I. INTRODUCTION

The fast development of technological applications based on magnetic systems in the past years, e.g., magnetic data storage devices, causes a high interest in thin magnetic films. One precondition for the technological development is the investigation of magnetic anisotropies and spin reorientation transitions connected therewith. Those reorientation transitions can occur from out of plane to in plane or vice versa for increasing film thickness d,[1] temperature T,[2–8] or external field B_0.

Quantum Monte Carlo (QMC) calculations give the possibility to compare numerically exact results with analytical approximations. In Ref. 9, the authors investigated a ferromagnetic monolayer including positive second-order anisotropy (easy axis perpendicular to the film plane). They discuss the temperature dependence of the magnetization $\langle S_z \rangle \times(T)$, as well as field induced reorientation transitions from out of plane to in plane and compare the QMC results with Green function theory (GFT). They found good agreement in the case of applied external field in the easy direction (here z axis). However, their GFT fails for external field applied in arbitrary direction, especially in the hard direction (within the film plane). As shown in Ref. 10, to obtain results closer to the QMC results for magnetic-field induced reorientation from out of plane to in plane, a more careful treatment of the local anisotropy terms is needed. In Refs. [10–13], a decoupling scheme was presented which yields excellent agreement with QMC results for out-of-plane systems.

The availability of theories such as GFT and their check against state-of-the-art numerical algorithms is highly desirable because of the size limitations of systems where QMC can be performed. On the other hand, the extension of GFT from a monolayer (where it can be compared to QMC as in the present work) to multilayer systems is a straightforward task without further approximations.[11]

Up to now, to our knowledge, there is no comparison between QMC and approximative theories for easy-plane systems and it is not obvious that the theory presented in Refs. [10–13] can reproduce the QMC results for in-plane systems as accurately as for the out-of-plane case. In contrast to the easy-axis case where a certain direction is preferred by the single-ion anisotropy, in easy-plane systems, the full xy plane is favored and no particular direction is distinguished within the plane. A magnetic field applied perpendicular to the plane does not destroy the xy symmetry.

For systems exhibiting this kind of symmetry, it was shown in a classical treatment that for external fields smaller than a critical field $0 \leqslant B < B_{crit}$ $(B \| z)$, stable vortices, i.e., a noncollinear arrangement of spins, can exist.[14–19] These vortices can undergo a Berezinskii-Kosterlitz-Thouless transition.[19] Depending on the strength of the anisotropy K_2, there might be vortices with or without a finite z component of magnetization.[14] In the small anisotropy case (which is considered in this work, $|K_2| < 0.1J$), there is a finite out-of-plane component, and for zero field, the two possible directions of magnetization $(\pm z)$ are energetically degenerate. For increasing magnetic field in the z direction, the vortices antiparallel to the field become more and more unstable (heavy vortices). However, the so-called light vortices (parallel to the field) are stable up to a critical field $B_z = B_{crit}$ and contribute a finite z component to the net magnetization of the considered system.[18]

The vortices in connection with a finite z component of the net magnetization emerge because of two reasons: first, the competition between the anisotropy (favoring an orientation of the magnetization within the xy plane) and the external field (favoring a perpendicular magnetization), and second, the xy symmetry of the system, which does not allow for a rotated homogeneous phase.

In this paper, we investigate both aspects, i.e., the field vs anisotropy competition, as well as the symmetry properties in detail for a *quantum-mechanical* system. We will compare the results of QMC and GFT calculations.

As explained in more detail below, the QMC algorithm used here allows only for an external field applied in the z

direction. Thus, the xy symmetry cannot be broken and no comparison between xy symmetric and asymmetric systems is possible. We will use GFT to clarify the influence of this symmetry breaking on the homogeneous phase. On the other hand, the GFT used here is by ansatz limited to the homogeneous phase. Therefore, it cannot describe a noncollinear (e.g., vortex) magnetic phase, which is expected for $B \| z$ and small field strengths. The breakdown of magnetization in GFT, as well as an exposed maximum in the magnetization in QMC at certain critical values of the external field or temperature, gives, however, a clear fingerprint of noncollinear configurations, at least if there is no metastable homogeneous phase. Below these critical values, there will be a finite z component in QMC *and* a vanishing magnetization in GFT.

For parameters where both theories are applicable, QMC serves as a test for the approximations needed in GFT.

In this work, we find indications for noncollinear spin configurations below a critical field or temperature for $B \| z$ by comparing results of QMC and GFT, as explained previously. Above the critical field, we obtain good agreement between QMC and GFT results. Breaking the xy symmetry by adding a small x component to the external field yields a stable collinear solution in GFT. The z component of the magnetization in this case is in good agreement with the QMC results calculated with untilted field. Thus, we can conclude that except for the restriction to collinear magnetic states, GFT describes the competition between external field and anisotropy quite well.

The paper is organized as follows. First, we explain the basics of the GFT and the QMC calculations. Then, we apply both approaches to easy-plane systems in external magnetic fields and report the results of our calculations.

II. THEORY

A. Green function theory

In the following, we present our theoretical approach using Green function theory. The focus of this work lies on the translational invariant system of a two-dimensional monolayer. Therefore, the following Hamiltonian is used:

$$H = -\frac{1}{2}\sum_{ij} J_{ij}\mathbf{S}_i\mathbf{S}_j - \mathbf{B}\sum_i \mathbf{S}_i - K_2\sum_i (S_{z,i})^2. \tag{1}$$

The first term describes the Heisenberg coupling J_{ij} between spins $\mathbf{S}_i$ and $\mathbf{S}_j$ located at sites i and j. The second term contains an external magnetic field $\mathbf{B}$ in arbitrary direction (the Landé factor g_J and the Bohr magneton μ_B are absorbed in $\mathbf{B}$). The third term represents second-order lattice anisotropy due to spin-orbit coupling. $S_{z,i}$ is the z component of $\mathbf{S}_i$ (the z axis of the coordinate system is oriented perpendicular to the film plane). The lattice anisotropy favors in-plane ($K_2 < 0$) or out-of-plane ($K_2 > 0$) orientation. Our Hamiltonian is similar to that used in Refs. 10, 11, 13, 20, and 21 for the investigation of the magnetic anisotropy and the field induced reorientation transition. To simplify calculations, we consider nearest neighbor coupling only,

$$J_{ij} = \begin{cases} J & \text{for } (i),(j) \text{ nearest neighbor} \\ 0 & \text{otherwise.} \end{cases} \tag{2}$$

The main idea of the special treatment presented in Refs. 10–13 is that, before any decoupling is applied, the coordinate system Σ is rotated to a new system Σ' where the new z' axis is parallel to the magnetization, implying a collinear alignment of all spins within the layer. Then, a combination of random-phase approximation[22] (RPA) for the nonlocal terms in Eq. (1) (Heisenberg exchange interaction term) and Anderson-Callen (AC) approximation[23] (AC) for the local lattice anisotropy term is applied in the rotated system. After application of the approximation, one gets an *effective* anisotropy

$$K_{eff}(T) = 2K_2\left(1 - \frac{1}{2S^2}[S(S+1) - \langle S_{z'}^2\rangle]\right)\langle S_{z'}\rangle, \tag{3}$$

where $\langle S_{z'}\rangle$ is the norm of the magnetization and S is the spin quantum number, which we have chosen to be $S=1$ in all our calculations.

As shown in comparison with an exact treatment of the local anisotropy term in Ref. 24, this approximation still holds up to anisotropy strengths $K_2 \sim 1/2J$. Therefore, we restrict ourselves in the following to small anisotropies ($K_2 \leqslant 0.1J$), as found in most real materials.[25] For a magnetic field applied in the xz plane [$\mathbf{B}=(B_x,0,B_z)$], our theory gives a condition for the polar angle θ of the magnetization:

$$\sin\theta B_z - \cos\theta B_x + K_{eff}\sin\theta\cos\theta = 0. \tag{4}$$

The uniform magnon energies ($\mathbf{q}=\mathbf{0}$) which dominate the physical behavior of the magnetic system can easily be extracted from the theory:[12,13]

$$E_{\mathbf{q}=\mathbf{0}}^2 = [\cos\theta B_z + \sin\theta B_x + K_{eff}(\cos^2\theta - \sin^2\theta)] \times (\cos\theta B_z + \sin\theta B_x + K_{eff}\cos^2\theta). \tag{5}$$

This result coincides with the spin-wave result[13] if one replaces $\langle S_{z'}\rangle$ by the spin quantum number S and K_{eff} by the bare anisotropy constant K_2 in Eq. (5). For an easy-plane system ($K_{eff} < 0$) with external field B in the z direction, the polar angle θ of the magnetization[26] is given by

$$\cos\theta = \begin{cases} -B/K_{eff}(T) & \text{for } B < |K_{eff}(T)| \\ 1 & \text{otherwise.} \end{cases} \tag{6}$$

By inserting Eq. (6) into Eq. (5), one immediately gets.

$$E_{\mathbf{q}=\mathbf{0}}^{K_{eff}<0}(B) = \begin{cases} 0 & \text{for } B < |K_{eff}(T)| \\ B + K_{eff}(T) & \text{otherwise.} \end{cases} \tag{7}$$

For gapless magnon energies $E_{\mathbf{q}=\mathbf{0}}=0$, the magnon occupation number ϕ diverges ($\phi \to \infty$) in film systems with ferromagnetic coupling $J>0$ and the magnetization becomes zero $\langle S_{z'}\rangle = 0$ in the collinear phase. This can be seen by following an argument of Bloch[27] already given in 1930. Since the spin-wave dispersion is $E \approx q^2$ in the vicinity of $\mathbf{q}=\mathbf{0}$, the spin-wave density of states $N(E)$ is independent of E for a two-dimensional system for E close to zero.[28] The excitation of spin waves at finite temperature leads to a variation of the magnetization of the order

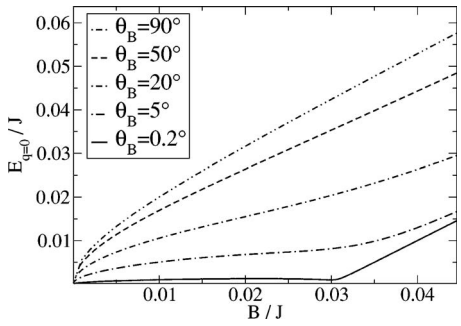

FIG. 1. The energies of the uniform magnon mode $E_{\mathbf{q}=\mathbf{0}}(B)$ for different polar angles θ_B of the external field. $E_{\mathbf{q}=\mathbf{0}}$ is zero below $B/J \approx 0.03$ for $\theta_B = 0°$. The prefactors $g_J \mu_B$ and k_B are absorbed in B and T, respectively. The latter are given in units of the nearest-neighbor Heisenberg coupling J. Parameters: $S=1$, $K/J=-0.03$, and $T/J=10^{-4}$.

$$\Delta m(T) \sim \int_0^\infty \frac{N(E)dE}{\exp(E/k_BT)-1} \sim k_BT \int_0^\infty \frac{dx}{\exp(x)-1}. \quad (8)$$

Since the integral in Eq. (8) diverges for $T \neq 0$ and excited spin waves lead to a reduction of the magnetization, one can conclude that the magnetization should be zero at finite temperature. However, for an infinitesimally small contribution of the external field parallel to the plane, i.e., $B_x \neq 0$, a finite gap in the excitation spectrum at $\mathbf{q}=\mathbf{0}$ opens. This can be seen in Fig. 1 where the uniform magnon modes $E_{\mathbf{q}=\mathbf{0}}(B)$ are shown for different orientations θ_B, where θ_B is the polar angle of the external field. The integral in Eq. (8) is now finite and a stable finite magnetization in the collinear phase having a well-defined orientation in the xz plane is possible.

Let us now come back to the case where the applied field is aligned in the z direction. It can be seen from Eq. (7) that for external field B $(B \| z)$ larger than a critical field $B > B_{crit}$ given by

$$B_{crit} = |K_{eff}(T,B)|, \quad (9)$$

a stable collinear solution exists. Since $K_{eff}(T)$ is a decreasing function of temperature T, a transition from noncollinear to collinear phase with increasing temperature is possible. In Fig. 2, we show the normalized critical field [Eq. (9)] B_{crit}/K_2 as a function of temperature T. For a constant magnetic field B $(B \| z)$ at a temperature T_1 with $B < K_{eff}(T_1,B)$, no stable collinear phase exists. Then, by increasing the temperature up to T_2, the effective anisotropy K_{eff} is sufficiently reduced such that $B > K_{eff}(T_2,B)$, and the collinear phase becomes stable. Before we come to the results, let us briefly sketch the main aspects of the QMC.

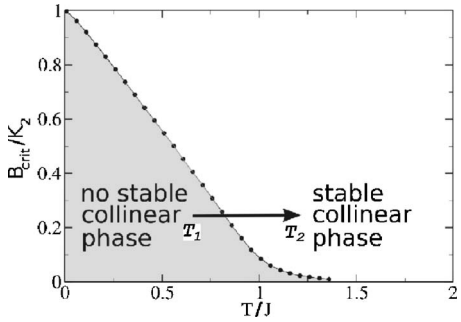

FIG. 2. The normalized critical field B_{crit}/K_2 as a function of temperature. Parameter: $S=1$.

B. QMC

In the previous section, we gave a short description of the theory used to treat a system described by a Hamiltonian of the form of Eq. (1). This theory applies to the thermodynamic limit (films of infinite size) but contains certain approximations. Additionally, the GFT is restricted to ordered phases with a collinear alignment of all spins. Therefore, it would be very useful to have exact results at hand to cross-check the predictions of GFT. A quantum Monte Carlo method particularly well suited for spin systems is the stochastic series expansion (SSE) with directed loop update. We will sketch this method here only briefly as detailed descriptions can be already found elsewhere.[29–31]

Our starting point is the series expansion of the partition function

$$Z = \mathrm{Tr}\, e^{-\beta H} = \sum_{n=0}^{\infty} \sum_{\alpha} \frac{\beta^n}{n!} \langle \alpha | (-H)^n | \alpha \rangle, \quad (10)$$

where H denotes the Hamiltonian, $\{|\alpha\rangle\}$ are basis vectors of a proper Hilbert space, and β is the inverse temperature. The Hamiltonian is then rewritten in terms of bond Hamiltonians:

$$H = -J \sum_{b=1}^{M} H_b, \quad (11)$$

where H_b can be further decomposed into a diagonal and an off-diagonal part:

$$H_{D,b} = C + S^z_{i(b)} S^z_{j(b)} + b_b [S^z_{i(b)} + S^z_{j(b)}] + k_{2b} [(S^z_{i(b)})^2 + (S^z_{j(b)})^2], \quad (12)$$

$$H_{O,b} = \frac{1}{2} [S^+_{i(b)} S^-_{j(b)} + S^-_{i(b)} S^+_{j(b)}]. \quad (13)$$

Here, we have renormalized the anisotropy constant k_{2b} and the magnetic field b_b in such a way that Eq. (11) coincides with Eq. (1). $i(b)$ and $j(b)$ denote the lattice sites connected by the bond b and the additional constant C in $H_{D,b}$ will be chosen such that all matrix elements of this term become positive, a condition necessary to interpret them as probabilities. Note that for a finite system at finite temperature the power series of the partition function can be truncated at a finite cutoff length Λ without introducing any systematic error in practical computations.[30] Therefore, reinserting Eq. (11) into Eq. (10) and rewriting the result yields

$$Z = \sum_{n=0}^{\Lambda} \sum_{S_{C_\Lambda}} \sum_{\alpha} \frac{\beta^n (\Lambda - n)!}{\Lambda!} \langle \alpha | S_{C_\Lambda} | \alpha \rangle. \quad (14)$$

Here S_{C_Λ} denotes a product of operators (operator string) consisting of n nonunity operators and $(\Lambda - n)$ unity opera-

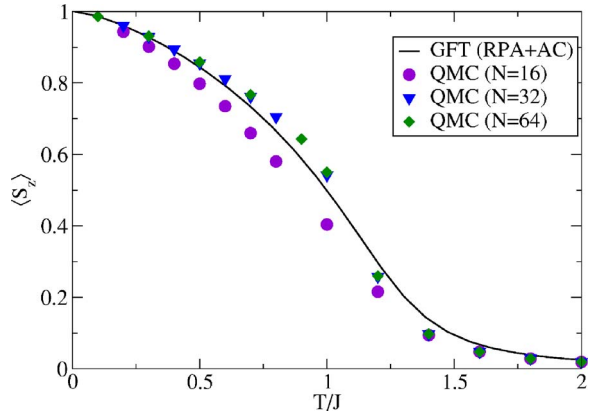

FIG. 3. (Color online) Magnetization vs temperature for an out-of-plane easy-axis system ($K_2>0$). Straight line: GFT (RPA+AC) result; symbols: QMC results for different system sizes N^2. Parameters: $S=1$, $B/J=0.01(B\|z)$, and $K_2/J=0.01$.

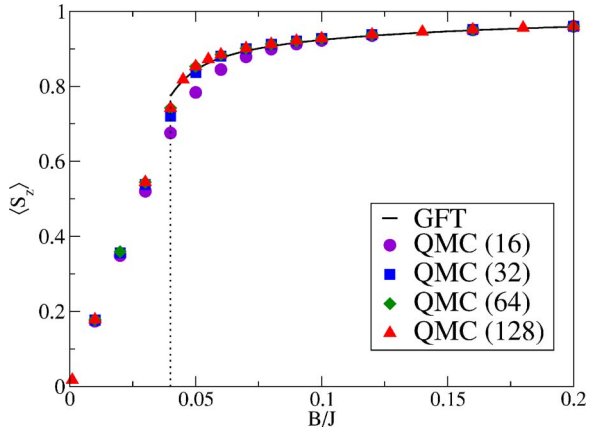

FIG. 4. (Color online) z component of magnetization as a function of external magnetic field for fixed temperature $T/J=0.4$. In contrary to the GFT the magnetization obtained by QMC remains finite for all fields. The QMC results are converged for $N\geqslant 64$. Parameters: $S=1$, $K_2/J=-0.06$ and $\theta_B=0°$.

tors $H_0=Id$, which were inserted to get operator strings of equal length Λ.

In fact, it is impossible to evaluate all operator strings in Eq. (14). The SSE-QMC replaces such an evaluation, therefore, by importance sampling over the strings according to their relative weight. Hence, an efficient scheme for generating new operator strings is needed. In the directed loop version of the SSE, this is done by dividing the update into two parts. In a first step, a diagonal update is performed by traversing the operator string and replacing some unity operators by diagonal bond operators and vice versa (the probabilities for both substitutions have to fulfill the detailed balance criterion). Then, the loop update follows in which new nondiagonal bond operators can appear in the operator string. For details of the update procedure, we refer the interested reader to the according literature.[29–31]

A full implementation of the SSE with directed loop update, which we have used for all QMC calculations in this work, can be found in the ALPS project.[31,32] Since the SSE-QMC used by us is implemented in z representation (spin quantization axis along the z axis), in-plane correlation functions, e.g., the in-plane magnetization, are not accessible. Further, $B\|z$ is the only possible field direction in the used QMC implementation because a traverse field (in-plane field component) would lead to nonclosing loops (see Ref. 9).

III. RESULTS

As mentioned in Sec. II A, the results for the in-plane systems are very sensitive to the effective anisotropy $K_{eff}(T)$. This sensitivity of the anisotropy is less pronounced for out-of-plane systems ($K_2>0$) since the applied field B ($B\|z$) and the intrinsic easy axis are parallel. In order to test our decoupling scheme (RPA+AC), we first compare GFT and QMC for an out-of-plane system.[33]

In Fig. 3, the magnetization $\langle S_z\rangle$ as a function of temperature T is shown. The straight line belongs to the GFT, whereas the symbols show the result of the QMC for different system sizes. Let us first comment on finite-size effects in the QMC results.

It can be seen in Fig. 3 that the QMC results converge for increasing system size N^2 (for $N\times N$ square lattice). Indeed, for $N\geqslant 32$, the QMC results are unbiased by finite-size effects and resulting magnetization curves are almost equal for increasing $N\geqslant 32$. Note that we have omitted error bars in the figures showing QMC results because the relative errors are of the order of 10^{-4}.

We now compare the GFT with the QMC results ($N=64$). For low temperatures ($T/J\leqslant 0.5$), we obtain excellent quantitative agreement. This is plausible because in this region, the GFT result coincides with the result of the spin-wave theory which is known to be reliable (exact for $T=0$) for low temperatures. For the intermediate region $T/J=0.5-1$, the RPA slightly underestimates the magnetization, which was also found in Ref. 9. The opposite is the case in the region near the extrapolated Curie temperature T_C,[34] where the magnetization is overestimated. The reason is the presence of longitudinal fluctuations, which play an important role in this region, and it is well known that the RPA fails to treat them properly.

We consider now the case of in-plane systems ($K_2<0$) and applied field in the hard direction ($B\|z$). As already mentioned, there is no "collinear" magnetization in the GFT for $B_z<|K_{eff}(T)|$. In Fig. 4, the z component of the magnetization is shown as a function of the external field B for a constant temperature $T/J=0.4$. As in Fig. 3, we see that the QMC results for $N\geqslant 64$ are almost converged and the finite size of the calculated system in QMC should not influence the results anymore. The dotted line marks a critical field B_{crit}. For magnetic fields larger than the critical one, $B>B_{crit}$, we obtain good agreement between QMC and GFT results. Below the critical field, $B<B_{crit}$, GFT does not yield a stable homogeneous magnetization. However, the QMC results show that there is a finite z component of the magnetization in the considered system for $0\leqslant B\leqslant B_{crit}$.

In order to compare QMC with GFT results, we have tilted the magnetic field by $\theta_B=0.5°$ which corresponds to $B_x<10^{-2}B_z$ in the GFT. As explained before, any symmetry breaking field $B_x\neq 0$ leads to a stable homogeneous magne-

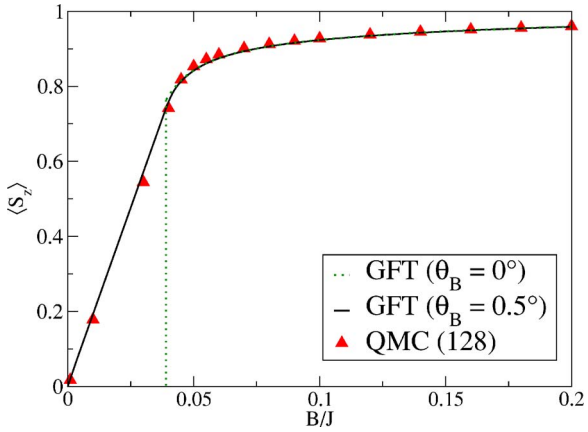

FIG. 5. (Color online) z component of magnetization vs external field for $T/J=0.4$ with slightly tilted field ($\theta_B=0.5°$) in the GFT result (solid line). The dotted line shows GFT result for ($\theta_B=0°$). Other parameters are as in Fig. 4.

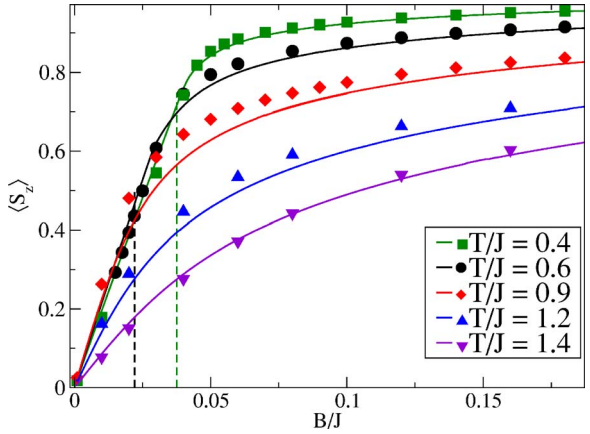

FIG. 6. (Color online) z component of magnetization vs external field for different temperatures T/J and fixed system size N^2 ($N=128$). Solid lines: GFT ($\theta_B=0.5°$); dashed lines: GFT ($\theta_B=0°$). Other parameters are as in Fig. 4.

tization with well-defined orientation in the xz plane. However, such a small contribution of the external field within the plane should hardly influence the z component of the magnetization. This is confirmed by Fig. 5 where we show QMC results ($N=128$, $\theta_B=0°$), as well as the corresponding GFT results with $\theta_B=0°$ and $\theta_B=0.5°$. As expected for $|B|>B_{crit}$, the two solutions in the GFT are nearly the same and agree well with QMC. Below the critical field, only the solution with the slightly tilted field yields a stable homogeneous magnetization and its z component compares well with the QMC result in the untilted case.

The above results can be interpreted within a semiclassical picture of noncollinear vortex configurations which are stable below a critical field B_{crit} in the z direction and contribute a finite z component to the magnetization in the case of an applied field.[18] Despite the lack of direct, quantitative access to such states (or corresponding physical in-plane observables) within the QMC algorithm, they are included in principle and one can observe their consequences, namely, a finite z component of the magnetization below the critical GFT field. On the other hand, GFT can only describe homogeneous collinear configurations of spins, therefore showing a breakdown of magnetization. However, by applying a small field in the x direction, the xy symmetry is broken and the spins rotate in the field direction (the vortices vanish) and the collinear phase is retrieved. Our results corroborate this interpretation based on the classical picture. Let us emphasize that both, GFT for slightly tilted field and QMC for $B\|z$, describe the competition between the external field (which favors magnetization parallel to z) and the anisotropy (which favors in-plane magnetization). Comparing the z components of the magnetization for both cases, one can conclude that the ratio of the competing forces is comparable for QMC and GFT. This indicates that this competition is correctly taken into account in GFT.

In Fig. 6, the same field dependence of the z component of the magnetization is shown for different temperatures. We have plotted the result for the tilted field in the case of GFT; the point of breakdown in the untilted case is indicated by the dotted line. It can be seen that for higher temperatures, no breakdown of collinear magnetization occurs, meaning that the condition for the critical field $[B\leqslant|K_{eff}(T,B)|]$ is never fulfilled in this case. The discrepancies at intermediate temperatures ($T=0.9-1.2$) are due to the RPA decoupling in the GFT, as was discussed already.

In Figs. 7–9, the z-component of the magnetization is plotted as a function of temperature obtained by GFT (straight line RPA+AC), as well as QMC (symbols) for different system sizes and a constant applied magnetic field.

Let us first discuss the qualitative behavior of the magnetization as a function of temperature which is found in all three figures. For high T ($T\gg T_{crit}$), the magnetization is reduced by thermal fluctuations (where the tail of the curve above $T/J\approx 1.5$ is due to the applied external field). In the vicinity of T_{crit}, $T-T_{crit}\to 0^+$, a competition between two effects sets in and has a pronounced influence on the magnetization. On the one side, the effective anisotropy acts against the external field [$B_{eff}=B-|K_{eff}(T)|$, $(B\|z)$]. The effective anisotropy $K_{eff}(T)$ is reduced with increasing temperature T and thus the effective field B_{eff} increases with T. This effect tends to enhance the magnetization with T. On the other side,

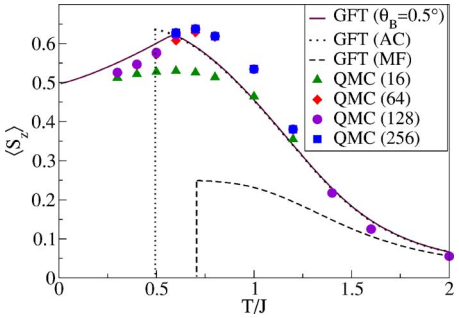

FIG. 7. (Color online) The z component of magnetization as function of temperature for a fixed external field. Below a critical temperature T_{crit}, there is a breakdown of magnetization in GFT where there is none in QMC. Parameters: $B/J=0.03$, $S=1$, and $K_2/J=-0.06$.

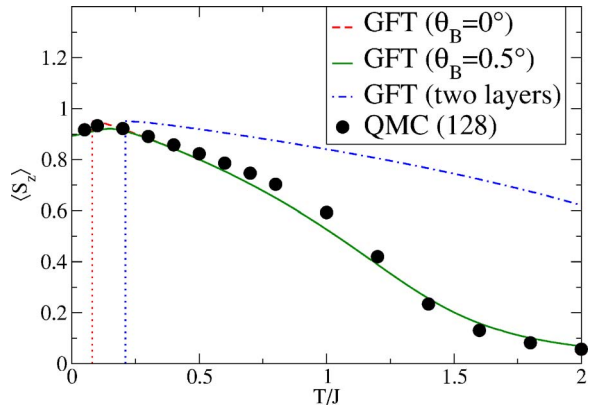

FIG. 8. (Color online) Same situation as in Fig. 7 for $K_2/J=-0.04$ (other parameters as in Fig. 7). The result for a two-layer film treated by GFT is also plotted (dashed-dotted line).

thermal fluctuations suppress the magnetization with increasing T. The flattening of the magnetization curve near T_{crit} is a result of this competition. For low temperatures $T<T_{crit}$, the effective anisotropy in the GFT cannot be overcome by the external field $[B<|K_{eff}(T)|, (B\|z)]$. Therefore, the collinear magnetization in our approximation vanishes due to the mentioned gapless excitations, in contrast to QMC which yields again a finite magnetization because noncollinear states are taken into account, as discussed above. The reduction of the z component of magnetization in QMC below T_{crit} can be pictured classically as the spins being in a noncollinear phase with an angle θ with respect to the z axis. Since, in general, anisotropy effects (which favor in-plane magnetization) increase when temperature is lowered, the z component of the magnetization decreases.

Now we discuss the three figures in detail. In Fig. 7, we have plotted QMC results for different system sizes showing again that these are well converged for $N\geqslant 64$. Thus, we conclude that the striking difference between GFT and QMC is not a mere finite-size effect. The breakdown of magnetization in GFT occurs at a critical temperature $T_{crit}/J=0.5$, whereas no such breakdown exists in QMC. However, the exposed maximum of the magnetization in QMC lies near the breakdown point. The differences between QMC and GFT in the temperature range $T/J\approx 0.3-1.3$ are due to the decoupling of the exchange and anisotropy term in GFT, as also seen in Fig. 3. It is worth mentioning that the value of the z component of the magnetization is nearly the same at the breakdown point in GFT and the maximum in the QMC. Thus, we have the result that although GFT cannot describe the noncollinear phase by ansatz, its breakdown coincides rather well with the onset of this phase, which we attribute to the maximum of the QMC curve. Figure 8 shows the same situation for a different anisotropy constant $K_2=-0.04$. The critical temperature is lower than in Fig. 7 since the ratio B_z/K_2 becomes larger. The tilted field case is also shown for the GFT results. Again, the qualitative agreement of the z component of magnetization with QMC is good. To confirm this point, we have plotted the temperature dependence for another set of parameters in Fig. 9. There is good qualitative agreement of the two approaches. Additionally, one gets a finite component in the x direction in GFT, which is also plotted in the figure. The two effects of the external field vs anisotropy competition are nicely to be seen: a noncollinear state for $B\|z$ (z component only in QMC but not in GFT) and rotation of magnetization for slightly tilted external field (seen only in GFT). The ratio of the competing forces agrees well again in both treatments.

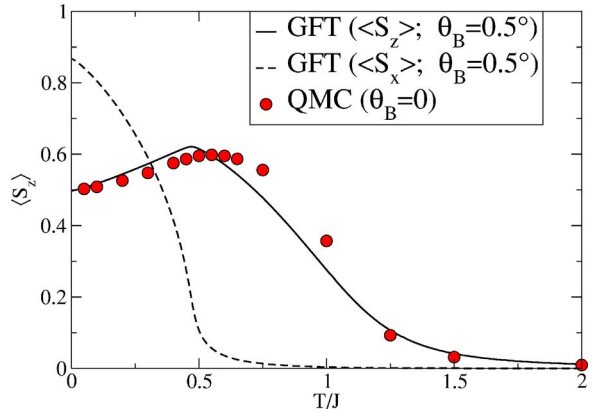

FIG. 9. (Color online) Same situation as in Fig. 7 for $K_2/J=-0.01$, $B/J=0.005$, and slightly tilted field ($\theta_B=0.5°$) for the GFT results.

In Fig. 7, we have plotted the results of a different decoupling scheme of the anisotropy terms (namely, a mean-field decoupling, dashed line in Fig. 7). Although the overall characteristic resembles the RPA+AC result (breakdown of magnetization), the mean-field results differ extremely from the QMC for a large range of temperature and underestimates the magnetization. This demonstrates the reliability of the Anderson-Callen treatment of the local anisotropy terms presented in Refs. 10, 12, and 13.

The extension of the GFT method to multilayer films is straightforward.[11] We have also included results for a two-layer film in Fig. 8 for the same parameters as in the monolayer case. One finds that for a double layer, magnetism is stabilized, which can be attributed to the increased coordination number and thus higher exchange energy. Just like for a monolayer, one observes a breakdown of collinear magnetization at some critical temperature. This is due to the fact that the same reasoning regarding the vanishing excitation gap also applies for multilayer (slab) systems.[35] The effective anisotropy *per layer* is essentially the same as for a single layer, thus, the critical $\langle S_z\rangle$ value (magnetization at critical field B_{crit}) is practically the same. The critical temperature is higher than that of a monolayer due to the increased magnetic stiffness of the double layer.

IV. SUMMARY AND CONCLUSIONS

Using GFT and QMC calculations, we studied easy-plane systems, as well as easy-axis systems with an external field applied perpendicularly to the film. The GFT treatment of the Hamiltonian in Eq. (1) consists of a RPA decoupling for the nonlocal terms and an AC decoupling for the local terms performed in a rotated frame, where the new z' axis is par-

allel to the magnetization. For the QMC calculations, we have used the SSE with directed loop updates, which is well suited for spin systems.

We have calculated the magnetization as a function of the external field, as well as temperature. We found a critical field and critical temperature, respectively, below which there is no magnetization in GFT whereas there is one in QMC. By tilting the field slightly in GFT so that it has a small component in the x direction, we get a stable magnetization even below the critical field or temperature. The z component of the magnetization in this case coincides well with the z component obtained by QMC for the untilted field, confirming that GFT and QMC agree well in the description of the external field vs anisotropy competition. However, this comparison can be only somewhat indirect, since QMC has access to the noncollinear ($B\|z$) state only, while GFT is limited to collinear ferromagnetic states (rotated homogeneous magnetization) found for slightly tilted external fields.

For parameters that are accessible by both QMC and GFT $[B\|z; B > B_{crit}(T)]$, QMC and GFT are in good agreement. Thus, one can conclude that the GFT is applicable to the homogeneous phases of systems described by Eq. (1) and can also be used for system configurations not accessible by QMC due to the too large system size, e.g., multilayer systems.

It would be an interesting task for a succeeding work to extend the GFT in order to get a deeper insight into the noncollinear configurations also.

APPENDIX: MAGNETIZATION ANGLE

Here we will discuss the second mathematical solution which occurs besides Eq. (6). For an external field in the z direction, the angle dependent part of the free energy including second-order anisotropy can be expanded as[1,36]

$$F = -M_z B_z \cos\theta - \tilde{K}_2 \cos^2\theta,$$

where M_z is the z component of the magnetization and $\tilde{K}_2$ is the first nonvanishing coefficient in an expansion of the free energy for a system with second-order anisotropy. For the equilibrium angle, one gets

$$\frac{\partial F(\theta)}{\partial \theta} = M_z B_z \sin\theta + 2\tilde{K}_2 \cos\theta \sin\theta \overset{!}{=} 0. \tag{A1}$$

Therefore, one gets two solutions for in-plane systems ($\tilde{K}_2 < 0$). For $\sin\theta \neq 0$, one gets immediately the solution of Eq. (6) if $2\tilde{K}_2/M_z \equiv K_{eff}$ holds. This is the stable solution. The trivial (second) solution $\sin\theta = 0$ is unstable for $B_z < |K_{eff}|$ because

$$\left.\frac{\partial^2 F(\theta)}{\partial \theta^2}\right|_{\sin\theta=0} = \begin{cases} <0 & \text{for } B_z < |K_{eff}| \\ >0 & \text{otherwise} \end{cases} \tag{A2}$$

holds. For a detailed discussion of stability conditions in film systems, we refer to Refs. 1 and 36.

*Electronic address: henning@physik.hu-berlin.de

[1] M. Farle, B. Mirwald-Schulz, A. N. Anisimov, W. Platow, and K. Baberschke, Phys. Rev. B **55**, 3708 (1997).
[2] A. Hucht and K. D. Usadel, Phys. Rev. B **55**, 12309 (1997).
[3] P. J. Jensen and K. H. Bennemann, Solid State Commun. **105**, 577 (1998), and references therein.
[4] R. P. Erickson and D. L. Mills, Phys. Rev. B **44**, 11825 (1991).
[5] D. K. Morr, P. J. Jensen, and K. H. Bennemann, Surf. Sci. **307-309**, 1109 (1994).
[6] P. Politi, A. Rettori, M. G. Pini, and D. Pescia, J. Magn. Magn. Mater. **140-144**, 647 (1995); A. Abanov, V. Kalatsky, V. L. Pokrovsky, and W. M. Saslow, Phys. Rev. B **51**, 1023 (1995).
[7] A. Hucht, A. Moschel, and K. D. Usadel, J. Magn. Magn. Mater. **148**, 32 (1995); S. T. Chui, Phys. Rev. B **50**, 12559 (1994).
[8] T. Herrmann, M. Potthoff, and W. Nolting, Phys. Rev. B **58**, 831 (1998).
[9] P. Henelius, P. Fröbrich, P. J. Kuntz, C. Timm, and P. J. Jensen, Phys. Rev. B **66**, 094407 (2002).
[10] S. Schwieger, J. Kienert, and W. Nolting, Phys. Rev. B **71**, 024428 (2005).
[11] S. Schwieger, J. Kienert, and W. Nolting, Phys. Rev. B **71**, 174441 (2005).
[12] F. Körmann, S. Schwieger, J. Kienert, and W. Nolting, Eur. Phys. J. B **53**, 463 (2006).
[13] M. G. Pini, P. Politi, and R. L. Stamps, Phys. Rev. B **72**, 014454 (2005).
[14] G. M. Wysin, Phys. Lett. A **240**, 95 (1998).
[15] E. Yu. Vedmedenko, A. Ghazali, and J.-C. S. Lévy, Phys. Rev. B **59**, 3329 (1999).
[16] K. W. Lee and C. E. Lee, Phys. Rev. B **70**, 144420 (2004).
[17] M. Rapini, R. A. Dias, and B. V. Costa, Phys. Rev. B **75**, 014425 (2007).
[18] B. A. Ivanov and G. M. Wysin, Phys. Rev. B **65**, 134434 (2002).
[19] J. M. Kosterlitz and D. J. Thouless, J. Phys. C **6**, 1181 (1973).
[20] P. J. Jensen and K. H. Bennemann, in *Magnetism and Electronic Correlations in Local-Moment Systems*, edited by M. Donath, P. A. Dowben, and W. Nolting (World Scientific, Singapore, 1998), p. 113.
[21] P. Fröbrich, P. J. Jensen, and P. J. Kuntz, Eur. Phys. J. B **13**, 477 (2000).
[22] N. N. Bogolyubov and S. V. Tyablikov, Sov. Phys. Dokl. **4**, 589 (1959).
[23] F. B. Anderson and H. Callen, Phys. Rev. **136**, A1068 (1964).
[24] P. Fröbrich and P. J. Kuntz, Phys. Rep. **432**, 223 (2006).
[25] Besides some rare-earth materials where the anisotropy can be of the order of J.
[26] For $B < |K_{eff}|$ there is another mathematical solution ($\sin\theta = 0$) which, however, is unstable (see Appendix).
[27] F. Bloch, Z. Phys. **61**, 206 (1930).
[28] P. Bruno, Phys. Rev. B **43**, 6015 (1998).

[29] A. W. Sandvik, Phys. Rev. B **59**, R14157 (1999).
[30] O. F. Syljuåsen and A. W. Sandvik, Phys. Rev. E **66**, 046701 (2002).
[31] F. Alet, S. Wessel, and M. Troyer, Phys. Rev. E **71**, 036706 (2005).
[32] ALPS collaboration, J. Phys. Soc. Jpn. **74**, 30 (2005) (source codes can be obtained from http://alps.comp-phys.org/).
[33] Note that a similar result has already been published in Ref. 9.
[34] Strictly speaking, there is no phase transition because of the applied magnetic field, as can be seen from the large tail of the magnetization curve. However, one can extract a T_C from the curves by extrapolating to the zero-field case and additionally to an infinite system size in the QMC calculations.
[35] A. Gelfert and W. Nolting, Phys. Status Solidi B **217**, 805 (2000).
[36] J. Lindner, Ph.D. thesis, Freie Universität Berlin, 2002.